REFERENCES

[1] K. M. Chen and B. S. Guru, "Induced EM field and absorbed power density inside human torsos by 1 to 500 MHz EM waves", Tech. Rep. no. 1, under NSF Grant ENG 74-12603, 1976.

[2] G. W. Hohmann, "Three-dimensional polarization and electromagnetic modeling, " *Geophys.*, vol. 40, pp. 309–324, 1975.

[3] N. Diffrient, A. R. Tilley, and J. C. Bardagjy, *Humanscale 1/2/3.* Cambridge, MA: M.I.T. Press, 1974.

[4] D. J. Morton, *Manual of Human Cross Section Anatomy.* (2nd edition), Baltimore, MD: Williams and Wilkins, 1944.

[5] A. C. Eycleshymer and D. M. Schoemaker, *A Cross-Section Anatomy.* New York: D. Appleton, 1911.

[6] C. C. Johnson and A. W. Guy, "Nonionizing electromagnetic wave effects in biological materials and systems," *Proc. IEEE*, vol. 60, pp. 692–718, 1972.

[7] C. C. Johnson, C. H. Durney, and H. Massoudi, "Long wavelength electromagnetic power absorption in prolate spheroidal models of man and animals," *IEEE Trans. Microwave Theory Tech.* vol. MTT-23, pp. 739–747, 1975.

[8] H. P. Schwan, "Electrical properties of tissue and cell suspensions," in *Advances in Biological and Medical Physics.* vol. V, J. H. Lawrence and C. A. Tobias, Eds., New York: Academic Press, 1957, pp. 147–209.

[9] D. M. Young, *Iterative Solution of Large Linear Systems.* New York: Academic, 1971.

[10] B. Carnahan, H. A. Luther, and J. O. Wilkes, *Applied Numerical Methods.* New York: Wiley, 1969.

[11] K. M. Chen and B. S. Guru, "Internal EM field and absorbed power density in human torsos induced by 1–500 MHz EM waves," *IEEE Trans. Microwave Theory Tech.*, vol. MTT-25, pp. 746–756, 1977.

[12] A. J. Poggio and E. K. Miller, "Integral equation solutions of three-dimensional scattering problems," in *Computer Techniques for Electromagnetics.* R. Mittra, Ed., New York: Pergamon, 1973, pp. 159–264.

[13] M. J. Hagmann, O. P. Gandhi, and C. H. Durney, "Upper bound on cell size for moment-method solutions," *IEEE Trans. Microwave Theory Tech.*, vol. MTT-25, pp. 831–832, 1977.

[14] W. Mendenhall and R. L. Scheaffer, *Mathematical Statistics with Applications.* North Scituate, MA: Duxbury, 1973.

[15] M. J. Hagmann, O. P. Gandhi, and C. H. Durney, "Improvement of convergence in moment-method solutions by the use of interpolants," *IEEE Trans. Microwave Theory Tech.*, vol. MTT-26, pp. 904–908, 1978.

[16] C. C. Johsnon, C. H. Durney, P. W. Barber, H. Massoudi, S. J. Allen, and J. C. Mitchell, "Radiofrequency radiation dosimetry Handbook," USAF Rep. SAM-TR-76-35, 1976.

[17] O. P. Gandhi, K. Sedigh, G. S. Beck, and E. L. Hunt, "Distribution of electromagnetic energy deposition in models of man with frequencies near resonance," in *Biological Effects of Electromagnetic waves*, selected papers of the USNC/URSI annual meeting, Boulder, CO, Oct. 20–23, 1975, vol. II, C. C. Johnson and M. L. Shore, eds.; HEW Publication (FDA) 77-8011, U.S. Government Printing Office, Washington, DC 20402.

[18] O. P. Gandhi, E. L. Hunt, and J. A. D'Andrea, "Electromagnetic power deposition in man and animals with and without ground and reflector effects," *Radio Sci.*, vol. 12, no. 6(S), pp. 39–47, 1977.

Head Resonance: Numerical Solutions and Experimental Results

MARK J. HAGMANN, MEMBER, IEEE, OM P. GANDHI, FELLOW, IEEE, JOHN A. D' ANDREA, AND INDIRA CHATTERJEE, STUDENT MEMBER, IEEE

Abstract—**We have used numerical solutions and experiments with phantom models of man, and experiments with the Long Evans rat to show the existence of head resonance. Greatest absorption in the head region of man occurs at a frequency of about 375 MHz. Absorption is stronger for wave propagation from head to toe than it is when the electric field is parallel to the long axis. The highest absorption cross section for the human head is projected to be approximately 3.5 times its physical cross section.**

I. INTRODUCTION

WE HAVE previously reported numerical solutions for the deposition of electromagnetic energy in a realistic model of man which showed the existence of resonances for body parts such as the head and arms, as well as for the whole body [1]. Further work has been done regarding head resonance, since we believe the phenomenon may be important in the study of behavioral effects, blood-brain barrier permeability, cataractogenesis, and other microwave bioeffects.

Our results show that the first resonance of the intact human head occurs at a frequency of about 375 MHz and has an S parameter (ratio of absorption cross section to physical cross section) of about 3.5 for incident plane waves propagating from head to toe. Earlier calculations for a spherical model of the isolated human head showed a geometrical resonance with $S = 1.1$ near 450 MHz, and a second resonance with $S = 1.4$ occurring near 2.1 GHz when allowance is made for the inhomogeneous structure by using a multilayered model [2]. The results of our study

Manuscript received October 16, 1978; revised February 23, 1979.

The authors are with the Departments of Electrical Engineering and Bioengineering, University of Utah, Salt Lake City, UT 84112.

0018-9480/79/0900-0809$00.75 ©1979 IEEE

suggest that the absorption in the head region is strongly dependent on the presence of the rest of the body.

In the following sections of this paper, we present new data regarding resonance of the intact human head obtained using both numerical solutions and phantom models for man, as well as experimental results for the Long Evans rat.

II. Numerical Solutions

Fig. 1 illustrates a realistic model of man which we used in earlier computations showing head resonance [1]. The model was obtained by using a total of 180 cubical cells of various sizes to obtain a best fit of the contour on diagrams of the 50th percentile standard man [3]. All numerical solutions reported in this paper are for a model having more detailed modeling of the neck and head, as shown in Figs. 2 and 3. Representation of the rest of the body is as shown in Fig. 1. Note that the number of cells has been increased from 12 to 144 in the head region, and from 4 to 32 in the neck region for a whole body total of 340 cells.

We have used a moment-method solution of the electric field integral equation with a pulse function basis and delta functions for testing [1] and an interpolant follow-up for improvement of convergence [4]. Since there are three unknown field components per cell, even using one plane of symmetry of the model the matrix is 510×510 complex, which corresponds to a system of 1020 simultaneous equations in 1020 real unknowns. Noniterative matrix solutions are required since the matrix has at least one complex eigenvalue having a real part with magnitude exceeding unity [5]. A total of 17 h of dedicated usage of a PDP-10 digital computer was required for each solution. Fortunately, weak diagonal dominance which is inherent in the matrix formulation contributes to the conditioning to allow reasonable round-off errors with such a large matrix size.

Figs. 4 and 5 show the head and whole-body specific absorption rate (SAR) calculated for the new model of man in free space with an incident plane wave having two different polarizations. Note that head resonance is more pronounced when the propagation vector is parallel to the body axis ($\vec{k} \| \hat{L}$) with propagation from head to toe than it is when the electric field is parallel to the long axis ($\vec{E} \| \hat{L}$). Experimental data for the Long Evans rat, described in Section IV of this paper, also suggest that head resonance is stronger for $\vec{k} \| \hat{L}$ than for $\vec{E} \| \hat{L}$ polarization. Some experimental data obtained using biological phantom models of man are presented for comparison in the next section of this paper.

Figs. 6 and 7 illustrate the distribution of absorbed energy in the head region near head resonance. The presence of a hot spot exists near the center of the head which is also seen in the distribution at the geometrical resonance for a sphere [2]. The distribution shown in Figs. 6 and 7 is only approximate since a homogeneous model was used in all calculations.

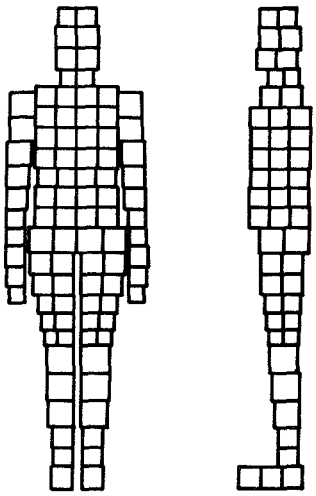

Fig. 1. Realistic model of man.

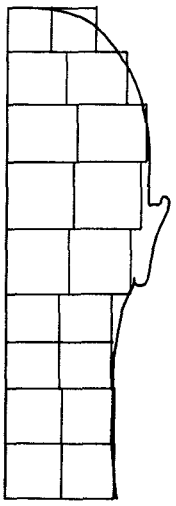

Fig. 2. Detailed modeling of the neck and head, front view.

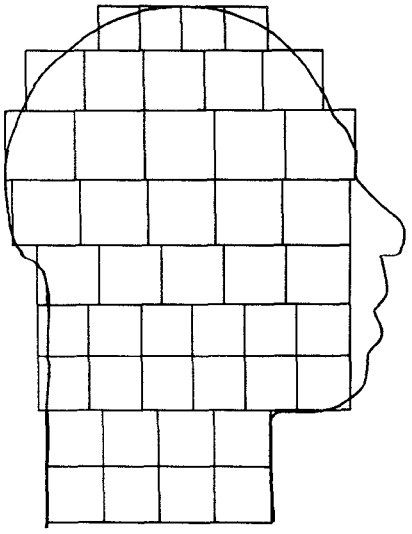

Fig. 3. Detailed modeling of the neck and head, side view.

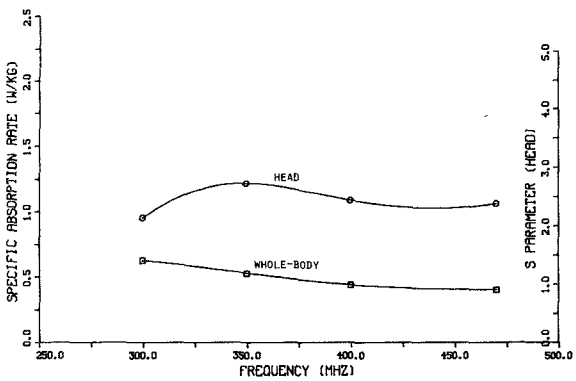

Fig. 4. Head and whole-body absorption for $\vec{E} \| \hat{L}$, propagation from front to back; incident intensity = 10 mW/cm^2.

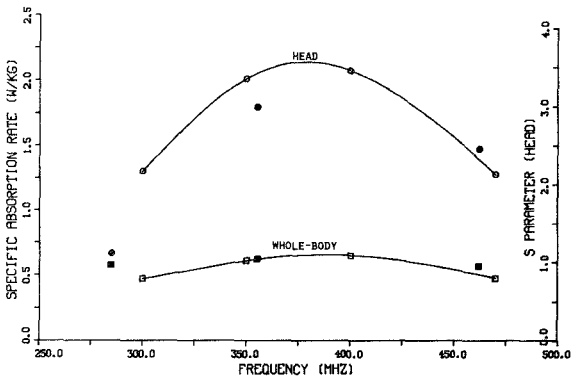

Fig. 5. Head and whole-body absorption for wave propagation from head to toe, $\vec{E}$ front to back; incident intensity = 10 mW/cm^2. Open markers are for numerical solutions and solid markers are for phantom models of man.

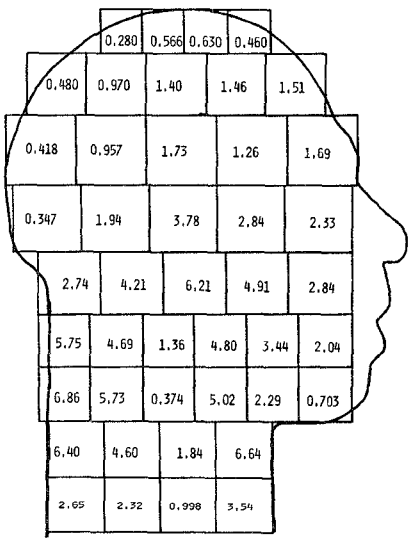

Fig. 6. Local SAR values, watts per kilogram for 10 mW/cm^2 incident fields. Inner layer of cells, 350 MHz, $\vec{k}$ head to toe, $\vec{E}$ front to back, whole-body average = 0.6132, head average = 2.014.

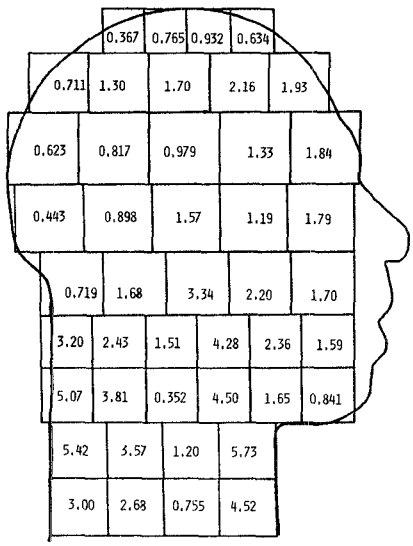

Fig. 7. Local SAR values, watts per kilogram for 10 mW/cm^2 incident fields. Outer layer of cells, 350 MHz, $\vec{k}$ head to toe, $\vec{E}$ front to back, whole-body average = 0.6132, head average = 2.014.

III. Experimental Results for Phantom Models of Man

We have used accurately scaled figurines [6] of 20.3-, 25.4-, 33.0-, and 40.6-cm length with biological phantom mixtures [7], described in Table I, to model the exposure of man to plane waves in free space. All values of absorbed dose were measured using a Thermonetics model 2401-A gradient layer calorimeter. Each figurine had the head attached to the torso by a layer of saline-soaked cloth, thus maintaining conductive contact but allowing easy separability for measurement of energy deposition in the head. For determination of the absorbed dose in the head, after separation, the part of the polyurethane mold holding the biological phantom material shaped in the form of the head was wrapped in Saran Wrap to limit loss of water by evaporation.

Table II gives the experimental values of SAR for figurines containing biological phantom mixtures and irradiated with propagation from head to toe. A plot of data from Table II on Fig. 5 shows good agreement between the numerical solutions and experiments with phantom models of man. The values in Table II suggest that for propagation from head to toe, the magnitude of absorption in the head region near head resonance is not strongly dependent on orientation of the $\vec{E}$ vector.

Both the numerical solutions in Section II and the phantom figurines have used homogeneous models. The next section of this paper presents experimental data obtained with the Long Evans rat.

IV. Experimental Results for the Long Evans Rat

Table III gives the experimental values of SAR for several tests made with both freshly killed and anesthetized Long Evans rats. The number of measurements (n)

TABLE I
COMPOSITION AND PROPERTIES OF PHANTOM MIXTURES. EXPERIMENTAL FREQUENCY = 2450 MHz

Figurine Length cm	Simulated Frequency MHz	Needed Whole-Body Average Values*		Composition of Phantom Material, %				Measured Properties	
		Permittivity	Conductivity mho/m	H_2O	Superstuff†	Polyethylene Powder	NaCl	Permittivity	Conductivity mho/m
20.3	284.5	37.3	7.76	75	10.90	7.61	6.49	36.0	7.61
25.4	355.6	36.7	6.40	75	10.38	9.75	4.87	35.1	6.23
33.0	462.3	36.3	5.11	75	10.40	10.62	3.98	34.4	4.96
40.6	569.0	36.1	4.25	75	11.00	11.25	2.75	35.8	4.14

* Whole-body average computed on the basis of 65 percent muscle, skin, and tissues with high water content and 35 percent fat, bone, and tissues with low water content using interpolation with data for these tissues from C. C. Johnson and A. W. Guy, "Nonionizing Electromagnetic Wave Effects in Biological Materials and Systems", *Proceedings of the IEEE*, Vol. 60, 1972, pp. 692-718.

† Superstuff obtained from Whamo Manufacturing Company, San Gabriel, California.

TABLE II
SAR* OF PHANTOM MODELS OF MAN FOR WAVE PROPAGATION FROM HEAD TO TOE

Frequency, MHz	$\vec{E}$ Front to Back		$\vec{E}$ Arm to Arm	
	Whole Body	Head	Whole Body	Head
285.0	0.578	0.669	0.827	0.999
355.6	0.624	1.797	0.691	1.498
462.3	0.572	1.479	0.558	1.244
569.0	0.478	0.750	0.394	0.702

* Watts/kg for 10 mW/cm^2 incident.

TABLE III
SAR* VALUES FOR THE LONG EVANS RAT

	$\vec{E} \parallel \hat{L}$		$\vec{k} \parallel \hat{L}$	
	Whole Body	Head	Whole Body	Head
Freshly killed rat (calorimeter)	27.36 n = 2	39.32 n = 2	28.34 ±1.41 n = 4	63.43 ±2.24 n = 4
Anesthetized rat (LCOF probe)	25.11 ±1.49 n = 4	30.97 ±1.58 n = 4	23.37 ±1.61 n = 4	34.40 ±1.69 n = 4

* Watts/kg (±SEM) for 95 mW/cm^2 incident at 2450 MHz.

and calculated standard errors in the measurements (SEM) are also given in the Table. Scaling suggests that head resonance for a medium-sized rat should occur near the test frequency of 2450 MHz.

The anesthetized rats were given a 45-mg/kg dose of sodium pentobarbitol to facilitate use of a fixed orientation and limit thermo-regulatory functions. Calorimetric measurements were used to determine the absorbed dose in the freshly killed rats. These measurements were made using a Thermonetics model 2401-A Seebeck envelope gradient layer calorimeter. The dose was also determined by measurement of the rate of increase in rat colonic temperature and brain temperature, using liquid crystal temperature optical fiber (LCOF) probes, in the anesthetized rats. For brain temperature the LCOF probe was implanted in a triphine hole 3 mm posterior to the Bregma cranial suture, 2 mm lateral to the midline cranial suture, and 6–8 mm below the top surface of the cortex.

The results in Table III show that head resonance is more pronounced for $\vec{k} \parallel \hat{L}$ than for $\vec{E} \parallel \hat{L}$ orientation which was also noted with the numerical solutions. Note that the ratio of head-to-whole-body heat content is less for the anesthetized rat than for the dead rat. Blood circulation may be reducing the relative magnitude of heating in the head region.

V. SUMMARY AND CONCLUSIONS

We have used three methods to study head resonance: numerical solutions, experiments with phantom models of man, and experiments with the Long Evans rat. All three approaches show the existence of head resonance. The phenomenon appears to have a greater magnitude for wave propagation from head to toe than for $\vec{E} \parallel \hat{L}$ orientation. For the former orientation the head absorption cross section as high as 3.5 times the physical cross section is projected.

The numerical solutions, which are supported by the experimental results for phantom models of man, suggest that the absorption is much stronger than would be predicted using a sphere to model the isolated head. The strong dependence on polarization would, of course, also be missed using a spherical model.

We believe that the enhanced absorption in the head region may make head resonance significant in the study of behavioral effects, blood-brain barrier permeability, cataractogenesis, and other microwave bioeffects.

REFERENCES

[1] O. P. Gandhi and M. J. Hagmann, "Some recent results on deposition of electromagnetic energy in animals and in models of man,"

presented at the USNC/URSI meeting, Airlie, VA, Oct. 30–Nov. 4, 1977. To be published in a special issue of *Radio Sci.* based on selected papers of the meeting.

[2] W. T. Joines and R. J. Spiegel, "Resonance absorption of microwaves by the human skull," *IEEE Trans. Biomed. Eng.*, vol. BME-21, Jan. 1974, pp. 46–48.

[3] N. Diffrient, A. R. Tilley, and J. C. Bardagjy, *Humanscale 1/2/3.* Cambridge, MA: M.I.T. Press, 1974.

[4] M. J. Hagmann, O. P. Gandhi, and C. H. Durney, "Improvement of Convergence in moment-method solutions by the use of interpolants," *IEEE Transactions on Microwave Theory and Techniques*, Vol. MTT-26, No. 11, November 1978, pp. 904–908.

[5] D. M. Young, *Iterative Solution of Large Linear Systems.* New York: Academic, 1971.

[6] O. P. Gandhi, E. L. Hunt, and J. A. D'Andrea, "Deposition of electromagnetic energy in animals and in models of man with and without grounding and reflector effects," *Radio Science*, vol. 12, no. 6(S), 1977, pp. 39–48, special issue based on selected papers of the 1976 USNC/URSI meeting in Amherst, MA.

[7] O. P. Gandhi and K. Sedigh, "Biological phantom materials for simulation at different frequencies," presented at the USNC/URSI meeting, Amherst, MA, Oct. 11–15, 1976.